Investigation on Silver Modification of Different Shaped Filler on the Heat Conduction Performance Improvement for Silicone Elastomer

Yifan Li[1,2]*, Yuan Zhang[1], Yicheng Liu[1], Huaqing Xie[1,2] and Wei Yu[1,2]*

[1]School of Energy and Materials, Shanghai Polytechnic University, Shanghai, China, [2]Shanghai Engineering Research Center of Advanced Thermal Functional Materials, Shanghai Polytechnic University, Shanghai, China

The continuous miniaturization and multi-function of electronic devices have put forward high requirements for the effective removal of the heat generated in the system. Developing thermally conductive polymer composite-based thermal interface materials is becoming the research hotspot. In addition to the usually concerned intrinsic thermal conductivity of the filler itself, surface modification is one of the important ways to form an effective heat conduction pathway and improve the overall thermal conductivity of materials. In this work, we used silicon rubber as the polymer matrix and achieved the thermal conductivity increment *via* various fillers with different shapes. The adopted fillers are spherical aluminum oxide (Al_2O_3), linear carbon fiber and boron nitride sheets, which can be considered as zero-dimensional (0D), one-dimensional (1D), and two-dimensional (2D) fillers respectively. We also prepared the silver-modified fillers and investigated the influence on the formation of heat conduction pathways and interfacial thermal resistance of different shaped fillers. An obvious increment in thermal conductivity of the composite with silver-modified fillers was observed compared to the composite with pristine fillers. Furthermore, through the practical thermal management performance investigation, we found the thermal conductivity increment did improve the actual heat transfer performance of composite elastomers functioning as thermal interface materials

Keywords: thermal conductivity, silicone elastomer, thermal fillers, silver treatment, interficial thermal resistance

INTRODUCTION

The continuous miniaturization of electronic devices causes localized heat accumulation, putting a high requirement for efficient heat removal. Polymeric-based materials are potential candidates for functioning as thermal interface materials (TIMs) due to their low cost, lightweight, easy process, and stable physical and chemical properties. Filler introduced technology is one of the most effective methods to improve the originally low intrinsic thermal conductivity of the polymer.

Thermal conductive polymer composites have experienced brilliant development in the past decade. From the initial composite system with a single filler to nowadays a multicomponent composite system designed with various strategies, the focus has shifted from a single increase in thermal conductivity to ensuring that other properties are not compromised (Guo et al., 2020; Zhang et al., 2020; Zhang et al., 2022). Except for the filler property itself, the filler content, distribution, and compatibility with the matrix are also essential in affecting heat conduction (Mehra et al., 2018; Orji

et al., 2018; Mehra et al., 2019). A lot of work emphasizes the compatibility of fillers with matrix materials since it plays an essential role in heat transfer, and interfacial engineering which aims at filler surface modification is the common method to approach this goal. Jia *et al.* prepared montmorillonite (MMT) containing silanization-reacted modifications with γ-Aminopropyltriethoxy silane (γ-APTES) and 3-(Glyoxypropyl propyl) Trimethoxy silane (GPTMS). They investigated the filler surface modification on the electrical and thermal properties of epoxy/MMT composites and found that the surface modification contributes to a better dispersion of nanoparticles, facilitating heat conduction (Jia et al., 2018). Kim *et al.* prepared thermally conductive Epoxy/boron nitride (BN) composites by different surface treatment methods (Kim and Kim, 2014). The results showed that the surface curing agent interrupted the interaction between the filler and the matrix and did not always improve the heat conduction Pan et al. introduced silane coupling agent KH550 modified hBN sheets into the PTFE matrix using the cold press sintering method. They investigated the effects of filler surface treatment on the morphology, thermal conductivity, and dielectric properties of the composites. The results indicated the interfacial bonding between h-BN and the PTFE matrix was improved after the surface modification, and the planar orientation of hBN in the PTFE matrix was reduced, which effectively improved the thermal conductivity (Pan et al., 2017). Zhang et al. prepared a new nano-flexible composite membrane by introducing γ-Aminopropyltriethoxy silane treated aluminum nitride (AlN) nanosheets with cellulose (CNF) nanofibers by vacuum filtration (Zhang et al., 2019). The results showed that the silane treatment reduced the phonon scattering between the interfaces of AlN and CNF substrates, and therefore, facilitate the heat conduction. Yu et al. designed a strawberry-like core-shell structure of alumina/ferric tannate/silver (Al_2O_3/TA-Fe^{3+}/Ag) nanoparticles and incorporated them into the nitrile butadiene rubber (NBR) matrix (Yu et al., 2021). The interfacial interaction and compatibility between the filler and the NBR matrix were enhanced, resulting in reduced phonon scattering and lower interfacial resistance.

The examples given above emphasize the interfacial engineering between filler and matrix, however, most of them were focused on a single filler system, and the effect of the same modification method for different shaped fillers on thermal conductivity is not taken into account. In addition, the correlation between interfacial engineering and thermal conductivity improvement lacks specific data support. Here in this work, out of consideration of the above two problems, we designed a silicone elastomer/filler composite system. Different shaped thermal fillers were adopted and interfacial engineering was realized by the surface silver treatment. Through a comprehensive theoretical investigation, we demonstrated that this surface silver treatment decreased the interfacial thermal resistance (ITR) and facilitate heat conduction. Meanwhile, we found that the effect of silver treatment on thermal conductivity improvement for different shaped fillers is not the same. Furthermore, the practical thermal management performance of the composite elastomer is investigated through a simulation approach. In this study, the surface treatment of different shaped fillers on the thermal conductivity improvement of polymer composite was observed, and the mechanism was elucidated in theory.

EXPERIMENTAL

Materials

The silicon rubber used was Sylgard 184 silicone Elastomer, purchased from Dow company. Aluminum oxide (Al_2O_3) was purchased from Lianrui New Material Co., LTD., carbon fiber (CF) was purchased from Chile Metallurgy Co., LTD., boron nitride (BN) was purchased from Xinzuan Alloy Material Co., LTD. (3-Glycidyloxypropyl) Trimethoxy silane (GPTS, >98%), functioning as the intermediate reagent for silver grafting, was purchased from Sigma. All of the reagents were of analytical grade and used as received.

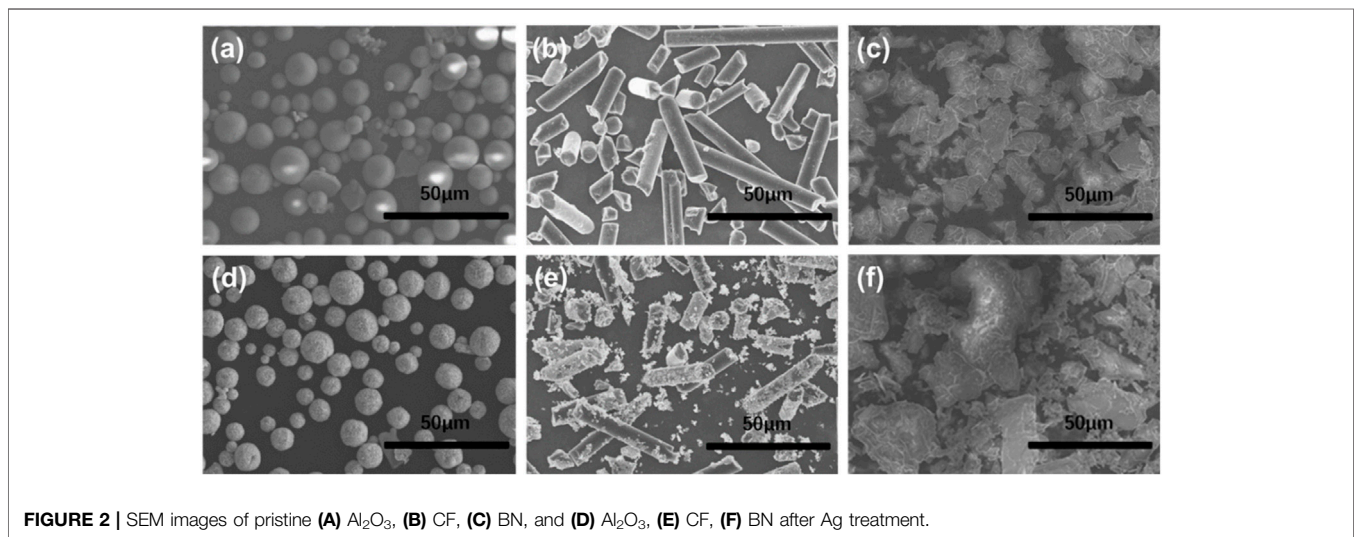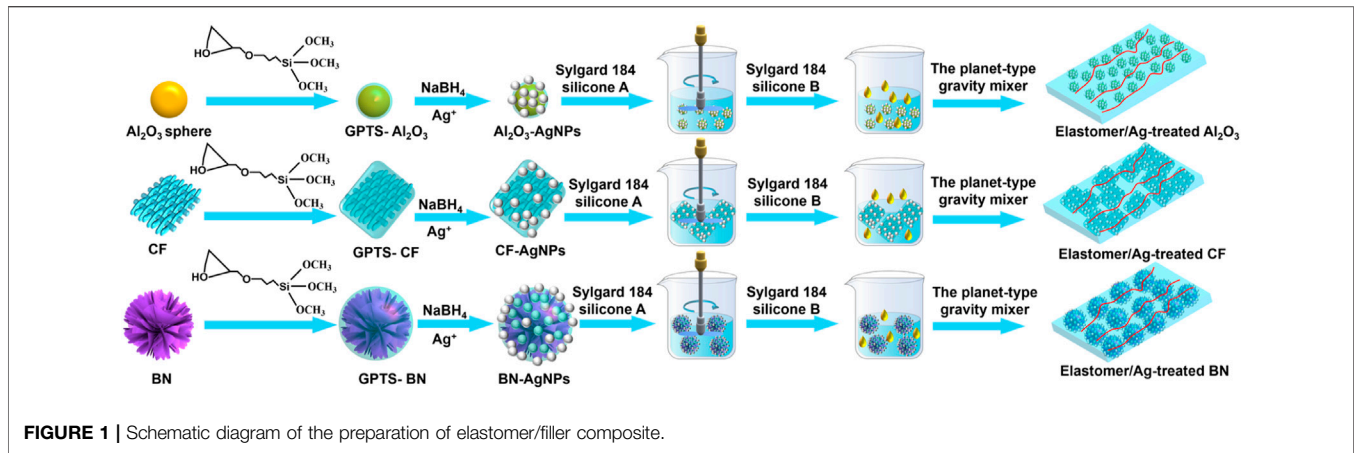## Surface Treatment of the Thermal Fillers

Surface treatment of the thermal filler includes two steps: surface modification of the filler and preparation of Ag-decorated fillers. Specifically, the thermal filler, absolute ethanol, and deionized water were mixed and placed under magnetic stirring for 1 h for the formation of a uniform dispersion. Then GPTS was added to the mixture and stirred for 2 h at room temperature. The mass ratio between the thermal filler and GPTS was controlled at around 50:1. It was then dried at 120°C for 2 h in the oven to evaporate the solvent. The dried powders were collected and marked as GPTS-filler. The powders were mixed with $AgNO_3$ and $NaBH_4$ solutions for the formation of Ag-decorated fillers. The concentrations of $AgNO_3$ and $NaBH_4$ were 0.01 mol L^{-1}. The volume ratio between $AgNO_3$ and $NaBH_4$ was controlled at 1:1.5. $AgNO_3$ was functioning as the Ag source and $NaBH_4$ was functioning as the reducing agent. The suspension was treated by vacuum-assisted filtration and dried for 12 h at 50°C to obtain the silver-treated filler. The mass ratio between the introduced silver and corresponding filler was around 1:500.

Preparation of Silicone Elastomer/Filler Composite

The preparation of silicon rubber/filler composite includes the pre-mixing and curing. Different types of thermal fillers were firstly mixed with the Sylgard 184 silicone component A and the mixture was placed in the planet-type gravity mixer for the uniform mixing. Then component B was added to the mixture and they were mixed again with a high gravity mixer. For elastomer/Al_2O_3 composite, the filler loading was controlled at 1, 5, 10, 20, and 40 vol%. For elastomer/CF and elastomer/BN composites, the filler loading was controlled at 1, 5, 10, 20, and 35 vol%. The evenly mixed sample was poured into the mold and dried in an oven at 100°C for 45 min to obtain the cured composite elastomer. The whole preparation were illustrated in **Figure 1**.

Characterizations

The micro-morphology was characterized by an S-4800 scanning electron microscope (SEM) produced by Hitachi, The instrument

FIGURE 1 | Schematic diagram of the preparation of elastomer/filler composite.

FIGURE 2 | SEM images of pristine **(A)** Al_2O_3, **(B)** CF, **(C)** BN, and **(D)** Al_2O_3, **(E)** CF, **(F)** BN after Ag treatment.

was working under a scanning voltage of 20 kV and scanning current of 20 KA. Thermal conductivity was tested with a thermal conductometer (TCi, C-Thermal). The thermal conductivity meter adopts the transient plane heat source method, has the special high-precision unit instrument test and communication technology, employed the computer high-speed data processing technology to carry on the fast data acquisition of the probe, through the perfect mathematical model rapid calculation, can quickly test the accurate and reliable results. Infrared thermal images were collected by thermal imager (Ti400, Fluke).

RESULTS AND DISCUSSIONS

Micro-Morphology Characterization of Thermal Fillers

The micro-morphology of the different types of fillers was firstly investigated. **Figures 2A–C** show the SEM images of Al_2O_3, CF, BN, and **Figures 2D–E** show those fillers after Ag treatment. One can see that the distribution of Al_2O_3 particles is uniform, and most of them are perfectly spherical with an average diameter of around 14 μm,

Figure 2A. After Ag treatment, the Al_2O_3 surface is coated with dense silver particles, indicating the successful silver plating process, **Figure 2D**. CF is rod-shaped, smooth, and of varying lengths, **Figure 2B**. After Ag treatment, the CF surface is covered with enough silver particles, most CF surface is uniformly covered with silver, and a small amount of CF surface is uneven, **Figure 2E**. The pristine BN was shown as irregular clumps, **Figure 2C**. After Ag treatment, the silver particles are less coated with BN and mostly exist between the clumped BN sheets, **Figure 2F**. The SEM images confirmed the successful Ag coating processes.

Micro-Morphology Characterization of Composite Elastomers

The micro-morphology of composite elastomers was characterized to investigate the filler distribution in the elastomers. Specifically, **Figures 3A–C** show the SEM images of composite elastomers with pristine fillers while **Figures 3D–F** show the SEM images of composite elastomers with Ag-treated fillers. Most Al_2O_3 dispersed evenly in the composite elastomers and there is adequate contact with each other, which may lead to a favorable heat conduction pathway,
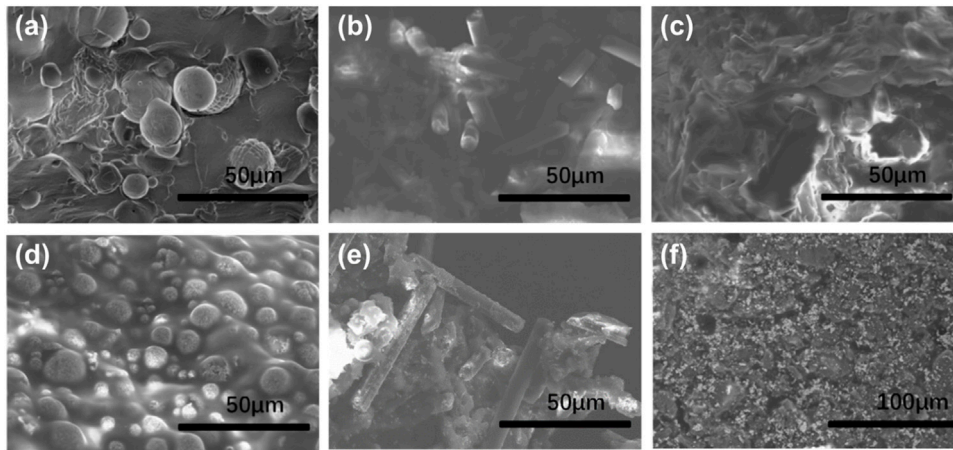
FIGURE 3 | SEM images of **(A)** elastomer/Al$_2$O$_3$ (40 vol%); **(B)** elastomer/CF (35 vol%); **(C)** elastomer/BN (35 vol%); **(D)** elastomer/Ag-treated Al$_2$O$_3$ (40 vol%); **(E)** elastomer/Ag-treated CF (35 vol%); **(F)** elastomer/Ag-treated BN (35 vol%).
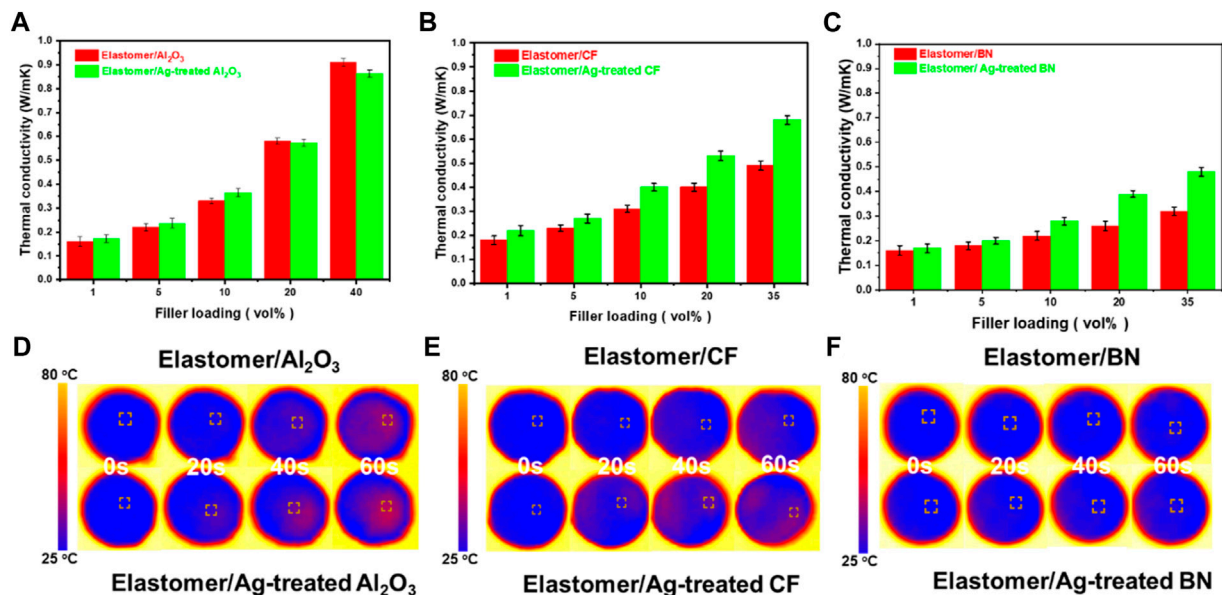

FIGURE 4 | Thermal conductivity comparison of **(A)** elastomer/Al$_2$O$_3$ and elastomer/Ag-treated Al$_2$O$_3$ with different filler loadings; **(B)** elastomer/CF and elastomer/Ag-treated CF with different filler loadings; **(C)** elastomer/BN and elastomer/Ag-treated BN with different filler loadings; FLIR images of **(D)** elastomer/Al$_2$O$_3$ and elastomer/Ag-treated Al$_2$O$_3$ (40 vol%); **(E)** elastomer/CF and elastomer/Ag-treated CF (35 vol%); **(F)** elastomer/BN and elastomer/Ag-treated BN(35 vol%) during a heating process.

Figure 3A. As shown in **Figure 3B**, CF is distributed in various directions with obviously observed space between fillers, which may affect the overall heat conduction. For elastomer/BN composite, BN is randomly distributed in the matrix, but there is sufficient contact between fillers, which can form a complete thermal conduction network, **Figure 3C**. It can be observed that Ag treatment would increase the surface roughness of the filler, bringing a better contact between fillers. The good contact mainly benefits from the silver surface modification, reflected by the increased roughness at the contact surface (Qiu et al., 2019). This influence on elastomer/Al$_2$O$_3$

is not that obvious since originally it has a relatively continuous heat conduction pathway. However, significant changes have been observed for elastomer/CF and elastomer/BN, identified by more space or holes filled in. Thus, the latter two may herald obvious thermal conductivity improvements after Ag treatment.

Thermal Conductivity Characterization

The thermal conductivity of the composite elastomers with pristine fillers and Ag-treated fillers is firstly tested to investigate the effect of the silver treatment on heat transfer
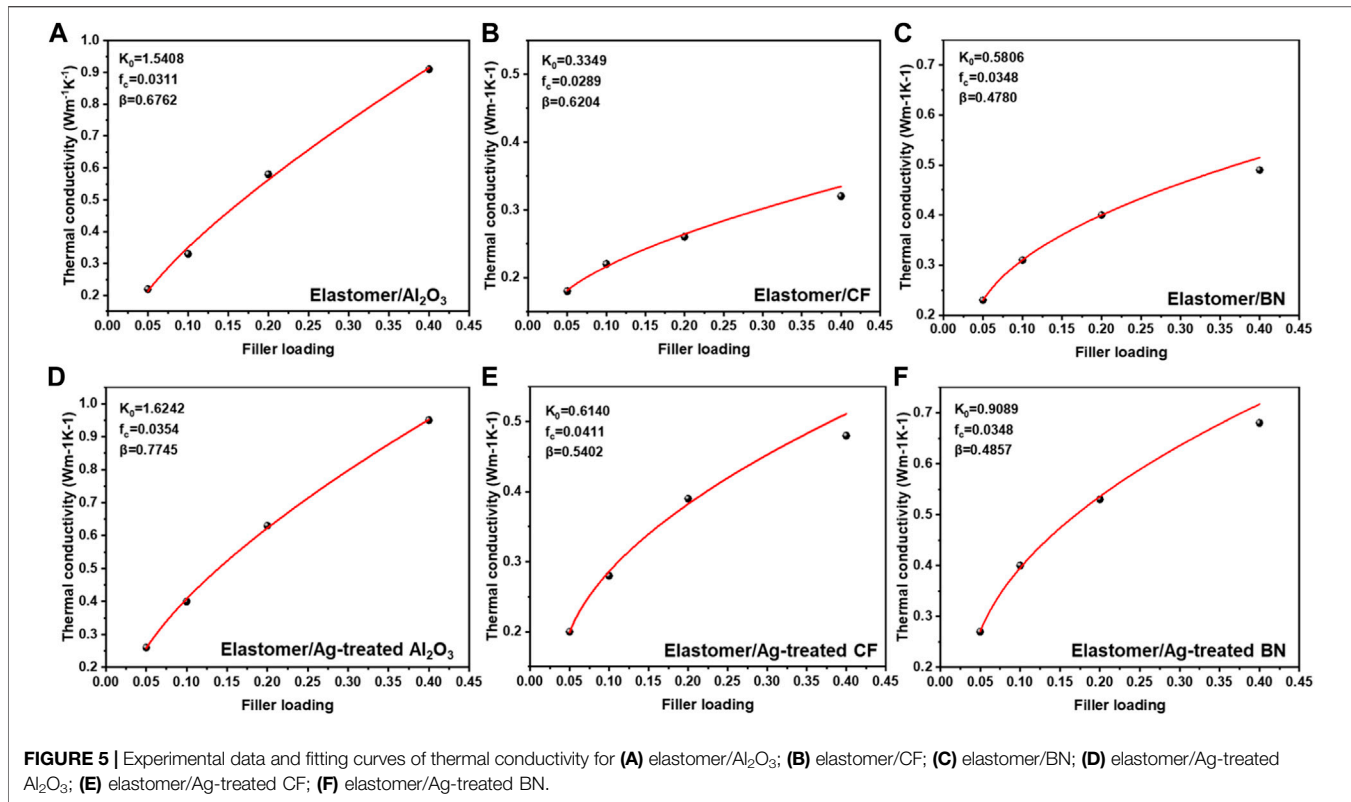
FIGURE 5 | Experimental data and fitting curves of thermal conductivity for **(A)** elastomer/Al$_2$O$_3$; **(B)** elastomer/CF; **(C)** elastomer/BN; **(D)** elastomer/Ag-treated Al$_2$O$_3$; **(E)** elastomer/Ag-treated CF; **(F)** elastomer/Ag-treated BN.

TABLE 1 | Tested thermal conductivity and calculated ITR for various composite elastomers.

Thermal filler		Al$_2$O$_3$	CF	BN
Thermal conductivity (W/mK)	Without Ag treatment	0.91	0.32	0.49
	With Ag treatment	0.95	0.48	0.68
Interfacial thermal resistance (K/W)	Without Ag treatment	7.58×10^6	7.30×10^6	1.83×10^6
	With Ag treatment	5.72×10^6	3.04×10^6	1.16×10^6

performance. **Figures 4A–C** show the thermal conductivity of composite elastomers with different loadings of various fillers before and after Ag treatment. It is worth mentioning that the highest volume loading concentration of Al$_2$O$_3$, CF, and BN in elastomer are 40, 35, and 35% respectively, while larger filler loadings would bring a dramatically increased viscosity and the final obtained elastomer composites are not uniform. Al$_2$O$_3$, CF, and BN have a similar thermal conductivity of ~37 W/mK, ~32 W/mK, and 33 W/mK, respectively. For original elastomers with intrinsic low thermal conductivity (0.15 W/mK), the influence of the thermal conductivity difference of these three fillers on the thermal conductivity of the final elastomer composite can be ignored. It is reported that the thermal conductivity of the composite is influenced by the filler thermal conductivity and filler/filler interfacial thermal resistance (ITR) and the latter is mainly decided by the distribution of the filler in the matrix. Thus, the thermal

conductivity difference of the final elastomer composite is mainly caused by the difference in ITR brought by various filler distributions. Owing to the relatively continuous heat conduction pathway in elastomer/Al$_2$O$_3$, it has the highest thermal conductivity compared to the other two.

The heat conduction ability of the composite elastomers is also studied by recording the temperature change during a heating process. The composite elastomers were placed on a heating plate with the initial temperature controlled at 100°C. **Figures 4D,E** capture the FLIR images of composite elastomers with the highest filler loading in 20-s intervals. The observed heat transfer ability is consistent with the thermal conductivity: the tendency of the temperature variation shows that heating rates took the following sequence: elastomer/Al$_2$O$_3$ > elastomer/CF > elastomer/BN. In addition, the Ag treatment facilities heat conduction and bring higher heating rates.

TABLE 2 | The parameters used in the simulation.

The volume of gravity (f$_i$)	9.81 m/ s^2
Dynamic viscosity (μ)	0.01 m/s
Total energy (E)	20 W
The heat source within the volume (S_h)	1.9×10^6 W/m^3
Stress tension (τ_{ij})	0
Anisotropic thermal conductivity of solid domains ($K_{eff}\nabla T$)	0
The apparent enthalpy (h)	151 J/g
The volume of density (ρ)	0.971 g/cm^3
Thermal conductivity of elastomer/Al$_2$O$_3$	0.91 W/mK
Thermal conductivity of elastomer/Ag-treated Al$_2$O$_3$	0.95 W/mK
Thermal conductivity of elastomer/CF	0.32 W/mK
Thermal conductivity of elastomer/Ag-treated CF	0.48 W/mK
Thermal conductivity of elastomer/BN	0.49 W/mK
Thermal conductivity of elastomer/Ag-treated BN	0.68 W/mK
The specific heat capacity of composites	1.46 kJ/kg K

Theoretical Investigation of Thermal Conductivity Improvement

The internal thermal resistance of the composite elastomer also plays an essential role in affecting its thermal conductivity. It is generally recognized that the interfacial thermal resistance (ITR) between adjacent fillers plays a critical role in affecting the overall internal thermal resistance of the composite, compared to the interfacial thermal resistance between filler and matrix (Ren et al., 2018). Several models have been proposed to describe the influence of ITR on the composite thermal conductivity, and here we used a nonlinear model developed by Foygel et al. to calculate the ITR (Foygel et al., 2005). The model is described by the following **Eq. 1**:

$$K - K_e = k_0 \left[\frac{(f - f_c)}{1 - f_c} \right]^\beta \qquad (1)$$

K_e is the thermal conductivity of the elastomer, K_0 is a pre-exponential factor ratio related to the thermal filler distribution, f_c is the critical volume content of the thermal filler and β is the conductivity exponent related to the aspect ratio of the thermal filler. The empirical values of K_0, f_c, and β can be figured out by fitting the experimental characterization data. **Figure 5** shows the fitting curves of experimental data of different composite elastomers and the value of each parameter is presented inside the figures.

Based on Foygel's model, ITR can be calculated by the following **Eq. 2**:

$$ITR = \frac{1}{K_0 d f_c \beta} \qquad (2)$$

In this equation, d is the specific size of the thermal filler which can be obtained from the SEM images, and K_0, f_c, and β are the parameters calculated from **Eq. 1**.

The tested thermal conductivity and calculated ITR for various composite elastomers are summarized in **Table 1**. The thermal conductivity improvement of elastomer/Al$_2$O$_3$, elastomer/CF, and elastomer/BN composites after Ag treatment are 4.3, 50.0,

and 38.7% respectively. As a comparison, the ITR decrement of elastomer/Al$_2$O$_3$, elastomer/CF, and elastomer/BN composites after Ag treatment are 32.5, 140.0, and 58.2% respectively. Thus one can conclude the degree of increase in thermal conductivity is mainly attributed to the degree of ITR decrement. The effect that surface silver treatment brings on the ITR decreasing of different-shaped fillers is different: it dramatically decreases the ITR of 1D CF and 2D BN adjacent fillers, while the influence for 0D Al$_2$O$_3$ sphere is not obvious since it originally has a relatively continuous heat conduction pathway. To sum up, the thermal conductivity improvements of silver modification on elastomers with different-shaped fillers are different: the surface treatment is more effective for 1D and 2D fillers, which is in good consistent with the previously reported literature. (Qiu et al., 2021).

Practical Thermal Management Performance Investigation

The practical thermal management performance of the composite elastomers is investigated by employing them to function as thermal interface materials (TIMs). Samples are placed between a heating plate and a heat sink, and the cross-interface temperature is used to represent the practical thermal management performance. Here we employ the finite element method (FEM) to simulate the working condition of TIMs and use ANSYS software to do the calculations. Specifically, a simplified geometric model considering convective boundary conditions is established in the software with reasonable external factors ignored. The mesh number is 4,843,459 with a minimized mesh size of 0.02 mm. For the steady-state heat transfer, the differential equation for thermal equilibrium is described by **Eq. 3**:

$$\frac{\partial}{\partial x}\left(k_x \frac{\partial T}{\partial x}\right) + \frac{\partial}{\partial y}\left(k_y \frac{\partial T}{\partial y}\right) + \frac{\partial}{\partial z}\left(k_z \frac{\partial T}{\partial z}\right) + q_v = 0 \qquad (3)$$

k_x, k_y, and k_z are the thermal conductivity in x, y, and z directions; q_v is the internal volume heat source, set as 1.9×10^6 W/m^3 in this case. The heat flux is set as 150 W/m^2, and the convection loads and temperature constraints are set as 50 W/m^{2}K and 20°C respectively. The governing equations include the continuity equation, momentum equation, and energy equation, listed as followed:

$$\text{Continuity equation}: \frac{\partial \rho}{\partial t} + \frac{\partial}{\partial x_i}(\rho u_i) = 0 \qquad (4)$$

$$\text{Momentum equation}: \frac{\partial}{\partial t}(\rho u_i) + \frac{\partial}{\partial x_j}(\rho u_i u_j)$$
$$= -\frac{\partial \rho}{\partial x_i} + \frac{\partial}{\partial x_j}\left[\mu\left(\frac{\partial u_i}{\partial x_j} + \frac{\partial u_j}{\partial x_i}\right)\right] + \rho f_i \qquad (5)$$

$$\text{Energy equation}: \frac{\partial}{\partial t}(\rho E) + \frac{\partial}{\partial x_i}[u_i(\rho E + p)]$$
$$= \frac{\partial}{\partial x_i}\left[k_i \frac{\partial T}{\partial x_j} + u_i(\tau_{ij})\right] + S_h \qquad (6)$$
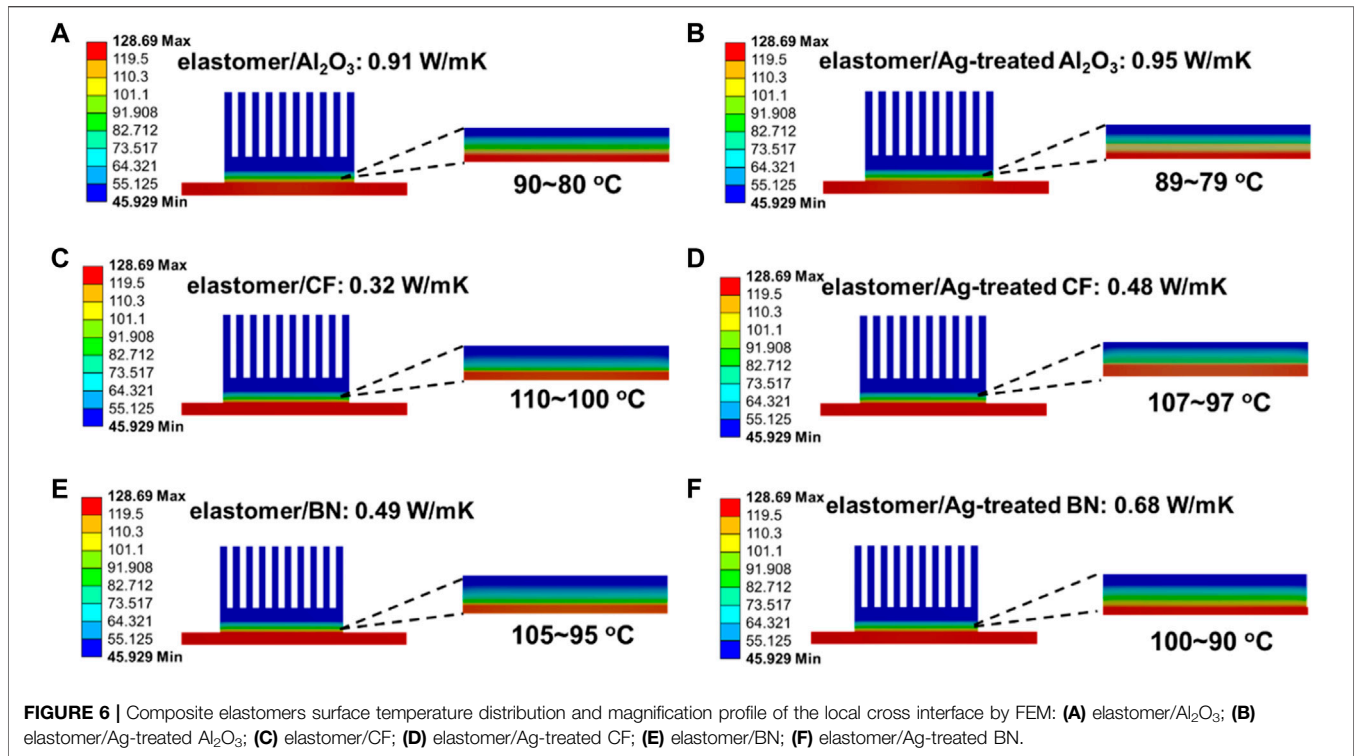
FIGURE 6 | Composite elastomers surface temperature distribution and magnification profile of the local cross interface by FEM: **(A)** elastomer/Al$_2$O$_3$; **(B)** elastomer/Ag-treated Al$_2$O$_3$; **(C)** elastomer/CF; **(D)** elastomer/Ag-treated CF; **(E)** elastomer/BN; **(F)** elastomer/Ag-treated BN.

f_i is the volume force that includes the gravity, μ is the dynamic viscosity, E is the total energy, $k_i \frac{\partial T}{\partial x_j}$ and $u_i (\tau_{ij})$ are transferred energy generated by heat conduction and viscous diffusion. τ_{ij} is the tensor of stress and S_h is the internal volume heat source considered as zero in this case. The heat conduction equation for calculating the solid domain is shown as followed:

$$\frac{\partial (\rho h)}{\partial t} + \nabla \cdot (V \rho h) = \nabla \cdot (K_{eff} \nabla T) + S_h \qquad (7)$$

$K_{eff} \nabla T$ is the anisotropic thermal conductivity of the solid domain, h is the apparent enthalpy, calculated by:

$$h = \int_{T_{ref}}^{T} c_p dT \qquad (8)$$

This simulation uses the mechanical APDL solver in Ansys for steady-state thermal analysis. The steady-state thermal analysis is a thermal analysis that is independent of time and the material parameters are only required for the thermal conductivity, after building the model, only the thermal physical parameters of the material need to be added and the temperature distribution is only related to the thermal contact between the materials. Therefore, the steady-state is different when the thermal conductivity is different and the thermal convection coefficient is the same, and the temperature distribution is different. The parameters used in the simulation was summarized in **Table 2**.

Figure 6 shows the simulated results including the overall view and the local magnification of the cross-interface. The yellowish plate surface corresponds to a lower temperature and thus a more efficient heat transfer process and excellent thermal management performance. The composite elastomers with Ag-treated thermal fillers have higher cross-interface temperatures than that with pristine thermal fillers. This phenomenon is particularly obvious for composites with CF and BN, which is mainly due to the greatly enhanced thermal conductivity. The above results demonstrate that the Ag modification on the thermal filler surface could improve the practical thermal management performance of the composite elastomers. According to the thermal conductivity improvement degree, the decrease of cross-interface temperature is approximately 1, 3, and 5°C for elastomer composite with 0D, 1D, and 2D fillers respectively.

CONCLUSION

To sum up, we perform the silver modification on the different shaped thermal fillers and introduced them into silicone elastomers. SEM characterizations confirm the successful Ag introduction in the composite system. Silver modification of filler with different shapes has different effects on thermal conductivity improvement. For elastomer composite with 0D Al$_2$O$_3$ filler, the increment is not obvious due to the originally existing continuous heat conduction pathway. For elastomer composite with 1D CF filler and 2D BN

filler, the increment is obvious. The further theoretical analysis demonstrates that the decreased filler/filler interfacial thermal resistance was responsible for this thermal conductivity improvement: elastomers with silver-modified 1D and 2D fillers exhibited a larger reduction of interfacial thermal resistance. The practical thermal management performance investigation indicates the increased thermal conductivity caused by silver treatment on filler surface is indeed beneficial to the heat dissipation of elastomer composites as thermal interface materials.

DATA AVAILABILITY STATEMENT

The original contributions presented in the study are included in the article/Supplementary Material, further inquiries can be directed to the corresponding authors.

REFERENCES

Foygel, M., Morris, R. D., Anez, D., French, S., and Sobolev, V. L. (2005). Theoretical and Computational Studies of Carbon Nanotube Composites and Suspensions: Electrical and Thermal Conductivity. *Phys. Rev. B* 71, 104201. doi:10.1103/physrevb.71.104201

Guo, M., Kashfipour, M. A., Li, Y., Dent, R. S., Zhu, J., and Maia, J. (2020). Structure-Rheology-Property Relationships in Double-Percolated Polypropylene/Poly (Methyl Methacrylate)/Boron Nitride Polymer Composites. *Compos. Sci. Technol.* 198, 108306. doi:10.1016/j.compscitech.2020.108306

Jia, Z.-R., Gao, Z. G., Lan, D., Cheng, Y. H., Wu, G. L., and Wu, H. (2018). Effects of Filler Loading and Surface Modification on Electrical and Thermal Properties of Epoxy/montmorillonite Composite. *Chin. Phys. B* 27, 117806. doi:10.1088/1674-1056/27/11/117806

Kim, K., and Kim, J. (2014). Fabrication of Thermally Conductive Composite with Surface Modified Boron Nitride by Epoxy Wetting Method. *Ceram. Int.* 40, 5181–5189. doi:10.1016/j.ceramint.2013.10.076

Mehra, N., Jeske, M., Yang, X., Gu, J., Kashfipour, M. A., Li, Y., et al. (2019). Hydrogen-bond Driven Self-Assembly of Two-Dimensional Supramolecular Melamine-Cyanuric Acid Crystals and its Self-Alignment in Polymer Composites for Enhanced Thermal Conduction. *ACS Appl. Polym. Mat.* 1, 1291–1300. doi:10.1021/acsapm.9b00111

Mehra, N., Li, Y., and Zhu, J. (2018). Small Organic Linkers with Hybrid Terminal Groups Drive Efficient Phonon Transport in Polymers. *J. Phys. Chem. C* 122, 10327–10333. doi:10.1021/acs.jpcc.8b01991

Orji, N. G., Badaroglu, M., Barnes, B. M., Beitia, C., Bunday, B. D., Celano, U., et al. (2018). Metrology for the Next Generation of Semiconductor Devices. *Nat. Electron.* 1, 532–547. doi:10.1038/s41928-018-0150-9

Pan, C., Kou, K., Jia, Q., Zhang, Y., Wu, G., and Ji, T. (2017). Improved Thermal Conductivity and Dielectric Properties of hBN/PTFE Composites via Surface Treatment by Silane Coupling Agent. *Compos. Part B Eng.* 111, 83–90. doi:10.1016/j.compositesb.2016.11.050

Qiu, L., Zhang, X., Guo, Z., and Li, Q. (2021). Interfacial Heat Transport in Nano-Carbon Assemblies. *Carbon* 178, 391–412. doi:10.1016/j.carbon.2021.02.105

Qiu, L., Zou, H., Wang, X., Feng, Y., Zhang, X., Zhao, J., et al. (2019). Enhancing the Interfacial Interaction of Carbon Nanotubes Fibers by Au Nanoparticles with Improved Performance of the Electrical and Thermal Conductivity. *Carbon* 141, 497–505. doi:10.1016/j.carbon.2018.09.073

Ren, L., Li, Q., Lu, J., Zeng, X., Sun, R., Wu, J., et al. (2018). Enhanced Thermal Conductivity for Ag-Deposited Alumina Sphere/epoxy Resin Composites through Manipulating Interfacial Thermal Resistance. *Compos. Part A Appl. Sci. Manuf.* 107, 561–569. doi:10.1016/j.compositesa.2018.02.010

Yu, L., Yang, D., Wei, Q., and Zhang, L. (2021). Constructing Strawberry-like Core-Shell Structured Al2O3 Nanoparticles for Improving Thermal Conductivity of Nitrile Butadiene Rubber Composites. *Compos. Sci. Technol.* 209, 108786. doi:10.1016/j.compscitech.2021.108786

Zhang, K., Lu, Y., Hao, N., and Nie, S. (2019). Enhanced Thermal Conductivity of Cellulose Nanofibril/aluminum Nitride Hybrid Films by Surface Modification of Aluminum Nitride. *Cellulose* 26 (16), 8669–8683. doi:10.1007/s10570-019-02694-5

Zhang, L., Pan, J., Cabrera, E. D., Garman, P. D., Wu, M., Li, Y., et al. (2020). Highly Oriented Graphitic Networks Grown by Chemical Vapor Deposition as Thermal Interface Materials. *Ind. Eng. Chem. Res.* 59, 22501–22508. doi:10.1021/acs.iecr.0c04519

Zhang, Y., Li, Y., Lei, Q., Fang, X., Xie, H., and Yu, W. (2022). Tightly-packed Fluorinated Graphene Aerogel/polydimethylsiloxane Composite with Excellent Thermal Management Properties. *Compos. Sci. Technol.* 220, 109302. doi:10.1016/j.compscitech.2022.109302

AUTHOR CONTRIBUTIONS

YLi: Conceptualization, Writing- original draft YZ: Methodology, Formal analysis YLiu: Methodology, Data curation HX: Resources, Validation WY: Writing review and; editing, Supervision, Project administration, Funding acquisition.

ACKNOWLEDGMENTS